PATTERN-BASED PRESSURE DROP OF AIR-WATER FLOW ACROSS A 90° SHARP MITER ELBOW

WAMEEDH AL-TAMEEMI[1, 2, *] PIERRE RICCO[1]

[1] *Department of Mechanical Engineering, The University of Sheffield, UK*
[2] *Reconstruction and Projects Office, Ministry of Higher Education and Scientific Research, Iraq*

ABSTRACT

Al-Tameemi, W. Ricco, P. "Pattern-based pressure drop of air-water flow across a 90° sharp miter elbow" Int. J. Comp. Meth. and Exp. Meas., Vol. 6, No. 1 (2018) 198-207

Air-water flow in a 90° sharp elbow (miter bend) is studied in a new purpose-built experimental facility at the University of Sheffield. For the first time, the two-phase flow is investigated in a miter bend for water-based Reynolds numbers Re_w=5600-12800 and water-to-air mass flow rate ratios $\dot{m}_w/\dot{m}_a$=10-3800. Four different flow patterns are observed in the upstream pipe (plug, slug, slug-annular and annular) by using high-speed high-resolution camera. The results show that the perturbation length upstream and downstream the elbow are significantly affected by the flow patterns. Two new values of the Lockhart-Martinelli parameter $\mathcal{C}$ are found for the pressure drop across the elbow.

Keywords: *two-phase flow, pressure drop,90° sharp elbow, flow patterns*

1 INTRODUCTION

Pipe fittings like elbows are common in many two-phase flow industrial applications and the prediction of pressure drop across these represents a very important fundamental and practical issue for piping system design. The prediction of pressure drop across elbows in two-phase flow is obviously more complicated than in single-phase flow due to many additional factors like the buoyancy force, which is mainly responsible for the two-phase flow patterns. An accurate prediction of flow patterns for different flow conditions is essential in two-phase flow investigations because the local pressure drop is strongly affected by the flow regimes[1],[2].

Flow patterns are influenced by many factors like flow orientation (horizontal or vertical), flow conditions (adiabatic or diabatic), and physical properties of the fluids. Although there are many empirical maps predicting the two-phase flow patterns in horizontal pipes, [3],[4] none of these maps can predict the flow patterns accurately for all flow conditions [1],[5].

Two-phase pressure drops in straight pipes $(\mathrm{d}P^*/\mathrm{d}Z^*)_{TP}$ were correlated by Lockhart and Martinelli [6] as follows:

$$(\mathrm{d}P^*/\mathrm{d}Z^*)_{TP} = \Phi_k^2 \, (\mathrm{d}P^*/\mathrm{d}Z^*)_k \,, \tag{1}$$

where k is the flow phase (liquid F or gas G) and Φ is the two-phase multiplier, expressed by Chisholm [7] as:

$$\Phi_F^2 = 1 + \frac{\mathcal{C}}{X} + \frac{1}{X^2}, \tag{2}$$

where $\mathcal{C}$ is an experimental parameter (given in table1) and X is the Martinelli pa-

* Email: wtal-tameemi1@sheffield.ac.uk

Table 1: Experimental values of the parameter $\mathcal{C}$ [7]

Liquid	Gas	$\mathcal{C}$
turbulent	turbulent	20
turbulent	laminar	12
laminar	turbulent	10
laminar	laminar	5

rameter defined as:

$$X^2 = \frac{(\mathrm{d}P^*/\mathrm{d}Z^*)_F}{(\mathrm{d}P^*/\mathrm{d}Z^*)_G}, \tag{3}$$

where $(\mathrm{d}P^*/\mathrm{d}Z^*)_F$ and $(\mathrm{d}P^*/\mathrm{d}Z^*)_G$ are single-phase pressure gradients in straight pipes for the liquid-phase and the gas-phase, respectively. Although this model was developed for two-phase pressure drop in round pipes, many studies [8–13] proved that the Lockhart-Martinelli model can be successful for different flow geometries by modifying the parameter $\mathcal{C}$. Other studies [9], [14] used the Lockhart-Martinelli model to fit pressure drop data of bubbly flow through 90° and 45° horizontal elbows.

In this study, we are motivated to investigate different air-water flow patterns in horizontal pipes upstream and across a sharp 90° elbow and to measure the pressure drop. Another crucial objective is to find the Lockhart-Martinelli parameters for the pressure drop across the elbow.

2 EXPERIMENTAL FACILITY AND PROCEDURES

A new experimental facility was designed and built for this work at The University of Sheffield. The facility consists of water and air lines, phase mixer and the test section fitted with the 90° sharp elbow. The facility is shown schematically in Fig. 1.

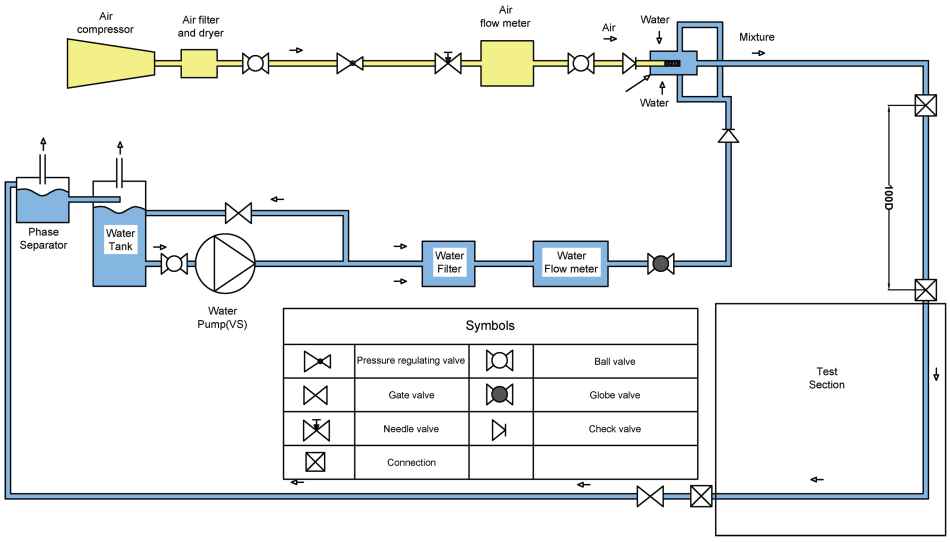

Figure 1: Schematic diagram of the test facility.

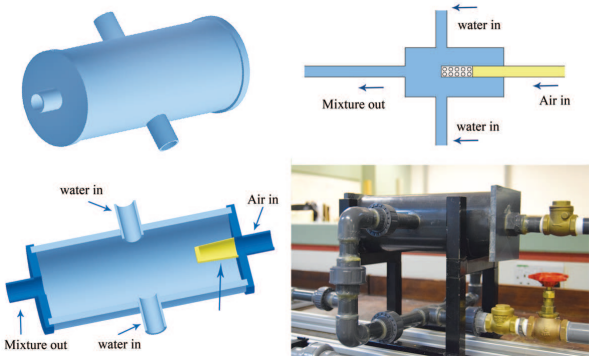

Figure 2: Schematic diagram and specifications of the phase mixer.

2.1 Water and Air Lines

Water is pumped from the storage water tank to the test section by using a variable speed pump with 80 LPM maximum flow rate at constant pressure. An automatic variable speed controller is used to obtain a constant pressure flow at variable flow rates. Two different water filters are located before the pump to minimize the intrusion of impurities in the test section. Water flow rates are measured by two different turbine flow meters (FTB-100 and FTB-104) to cover a wide range of water flow rates 1.3 - 13.5 LPM and 6.5 - 60 LPM, respectively. The flow meters were calibrated by the manufacturer with a $\pm 0.5\%$ flow reading accuracy. A six digits ratemeter (Omega DPF-702) is used to display the flow meters readings in LPM.

The high pressure (10bar) compressed air is supplied by an air compressor which is located outside the building. A pressure valve is used to regulate the air pressure to the required air flow rate. An air filter and dryer is located before the air flow meter to supply the test section with clean dry air. Air flow rates are measured by using an air mass flow meter (FMA-1612A-v2) 2.5-500 SLPM. The flow meter was calibrated by the manufacturer with an accuracies of $\pm 0.8\%$ of reading $+ \pm 0.2\%$ of FS.

2.2 Phase Mixer

An air-water phase mixer was designed and constructed for this work. Two jets of water enter the mixer from opposite sides and perpendicularly to the axis of the mixer. Air enters the mixer parallel to its axis through a section of porous media with 0.1mm holes diameters to obtain a smooth air stream. The two-phase mixture leaves the mixer from the opposite side of the air entrance as shown in Fig. 2.

2.3 Test Section

The test section was constructed from commercial acrylic pipes with 2mm wall thickness, 21 mm diameter, and $240D^*$ total length ($100D^*$ upstream and $140D^*$ downstream the elbow), where D^* is the pipe diameter. The section was assembled from segments which were joined together by using specially designed acrylic flanges. The 90° sharp angled elbow was constructed by cutting two pipe pieces accurately at a 45° angles and by welding them together using a special acrylic welding solution.

Ten measurements stations are located along the test section to measure the pressure distribution along the section, as shown schematically in Fig. 3. Pressure taps were designed for this work and they were machined from the same material of the

pipes. After fixing the taps in their locations, 1-mm holes were bored radially through the pipe wall to allow the fluid to flow out without perturbing the flow inside the pipe.

2.4 Data Acquisition

A differential pressure transducer (PX409-10WDWUI) calibrated by the manufacturer with ± 0.08 % FS BSL accuracy is used to measure the two-phase pressure drop along the test section. An absolute pressure transducer (PX309-100G5V) is used to measure the absolute pressure in the range of 0 - 6.8 bar absolute pressure range. It was calibrated by the manufacturer with ±0.25% FS BSL uncertainty. A National Instrument data acquisition system with 16-bit resolution and a dedicated Labview code are used for pressure measurements data logging. Flexible clear pipes with 6mm diameter connect the pressure transducers and the measurement stations.

Type K thermocouples are used with a Picco data logger to measure air and water temperatures at the beginning of each experiment. The thermocouples were calibrated carefully against an accurate thermometer with less than ± $0.5°C$ accuracy. The properties for air and water are calculated by using NIST Refprop software [15] by using the measured temperature and pressure for each experiment.

A Phantom v210 high-speed high-resolution camera is used to study the two-phase flow patterns in the straight pipe upstream of the elbow at 1750 FPS. A white acrylic plate with white LED light is employed as a monitor background to obtain optimum quality videos. The videos at different flow conditions are analyzed to distinguish the observed flow patterns at each flow condition.

2.5 Experimental procedure

All experiments are started by regulating the water flow rate to the needed value after recording the initial values of pressure and temperature. The connecting pipes between the measurement stations and the pressure transducers are then purged from any possible air bubbles. The preparation of the mixture is started after obtaining a steady state water flow by regulating the air flow rate to the needed value. The

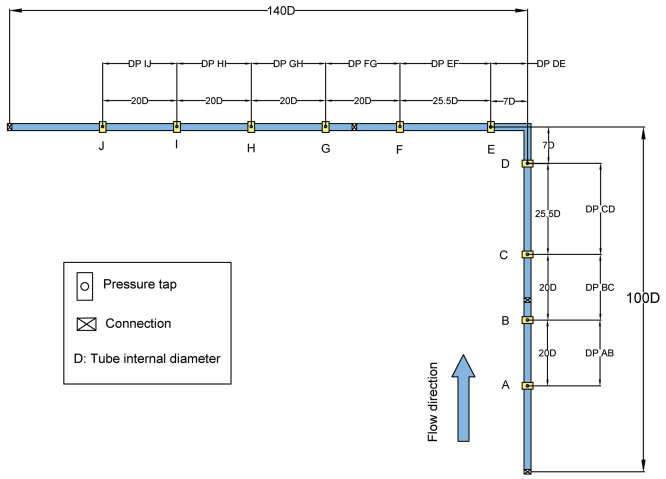

Figure 3: Schematic diagram of the test section.

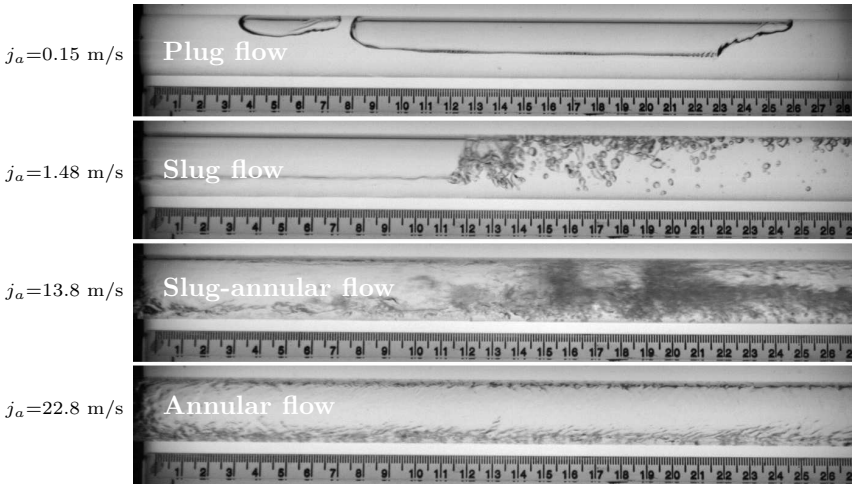

Figure 4: Flow patterns in horizontal pipe upstream the elbow for $j_w = 0.495$ m/s and different j_a values.

videos are then captured by the high-speed camera, and the pressure drop and the flow temperature are recorded. These steps are repeated at different water and air flow rates at all the measurement stations. Flows with five different water superficial velocities 0.297-0.678 m/s and 32 air superficial velocities 0.1485 - 24.75 m/s are studied in this work.

2.6 Uncertainty analysis

The square root of the sum of the sequence method (RSS) [**?**] is used for the uncertainty analysis. The measuring instruments are either calibrated by their manufacturers or in the lab, as clarified in section 2.4. The uncertainties in measured values (diameter, length, surface roughness and physical properties) are obtained by direct measurements. The pipe diameter is measured at five different locations by using a micrometer with ±0.1mm uncertainty. The length of the test section and the distances between the measurement stations are measured by using measuring tape with ± 1mm uncertainty, while the pipe surface roughness is measured by using a Dektak 150 surface profiler with ± 2% uncertainty. The angle of the assembled 90° sharp elbow is measured carefully by using a special protractor with ± 0.5° uncertainty. The maximum data uncertainties are indicated by error bars in the graphs of section 3.

3 EXPERIMENTAL RESULTS

For the first time, the two-phase pressure drop across a horizontal 90° sharp miter elbow for 143 different flow conditions is investigated. The experimental data for the flow visualization and pressure measurements are presented in this section.

3.1 Flow Visualization

Four different flow patterns (plug, slug, slug-annular and annular) are observed, as depicted in Fig.4. The flow patterns are divided into two groups: i) intermittent patterns, which include the plug and slug patterns, and ii) continuous patterns, which include the slug-annular and annular patterns. Fig.5 depicts a comparison between our experimentally observed flow patterns and Mandhane[4]'s predicting map for horizontal pipes. About 70% of the experimental flow patterns are predicted by the map.

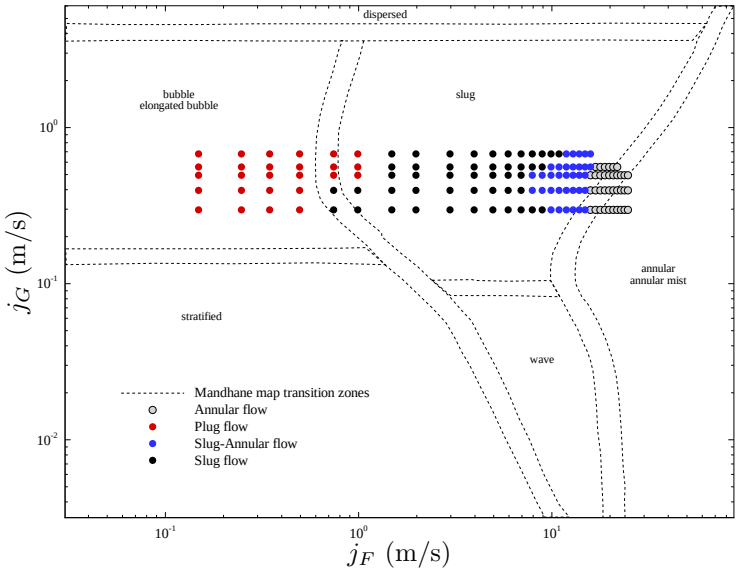

Figure 5: Mandhane map with the observed flow patterns experimental data.

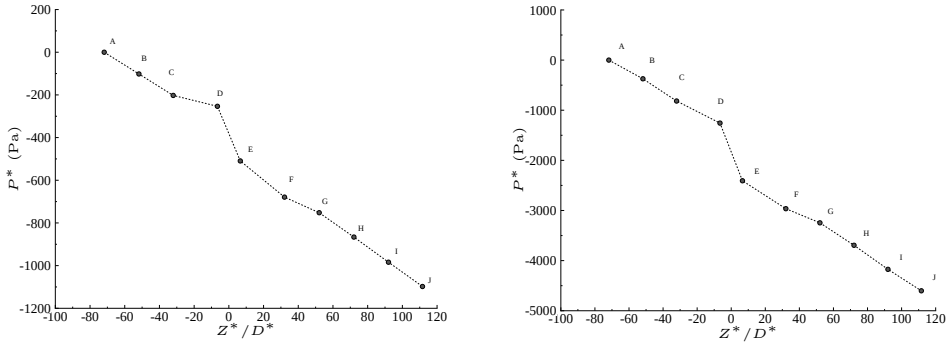

(a) Intermittent (plug) flow j_a=0.742 m/s .

(b) Continuous (annular) flow j_a=6.93 m/s .

Figure 6: Pressure distribution along the test section at j_w=0.4 m/s.

3.2 Pressure Distribution

Pressure is measured along the test section (relative to the first measurement station A, as shown in Fig. 3 across the 90° sharp elbow to quantify the flow perturbation lengths upstream and downstream of the elbow for different flow patterns. Fig.6a depicts the pressure distribution for an intermittent flow pattern case. The pressure increased slightly between stations C and D before dropping after station D upstream of the elbow. Downstream of the elbow, the effect of the elbow lasts longer than upstream of it and it disappears after station G.

The effect of the elbow upstream of the elbow starts from station D for continuous flow pattern as shown in Fig.6b, while the flow recovers after station G downstream of the elbow, similar to the effect on intermittent flow pattern case. The effect lasts longer upstream of the elbow in the intermittent flow pattern case than in the continuous flow pattern case. The elbow pressure loss is counted between stations C and

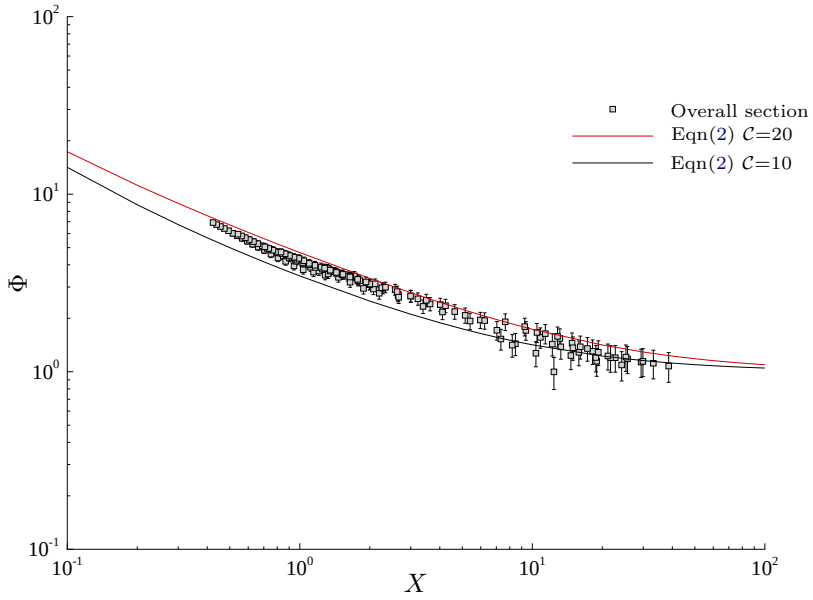

Figure 7: Pressure drop across the whole test section compared with eqn (2).

G for intermittent flow and between stations D and G for continuous flow patterns.

3.3 Pressure Drop in 90° Elbow

Fig.7 shows the scaled experimental pressure drop data fitted with the Lockhart-Martinelli correlation eqn.2 [6]. The pressure drop across the whole test section between stations A and J is well expressed by the model with $\mathcal{C} = 10 - 20$. We observe that our data are comprised between the correlation curves for $\mathcal{C} = 10$ and $\mathcal{C} = 20$.

The scatter is due to the additional factors generated by the elbow, such as severe flow separation and significant perturbation of the flow patterns.

The pressure drop per unit length $\mathrm{d}P^*_{TP}/\mathrm{d}Z^*$ in the elbow area is higher than across the whole section section and it is strongly affected by the flow patterns as depicted in Fig.8.

Therefore, we choose to use two $\mathcal{C}$ parameters, one corresponding to the intermittent patterns (slug and plug) and one corresponding to the continuous patterns (slug-annular and annular). The new values are $\mathcal{C} = 114 \pm 9.4\%$ for intermittent patterns and $\mathcal{C} = 80 \pm 2.9\%$ for continuous patterns.

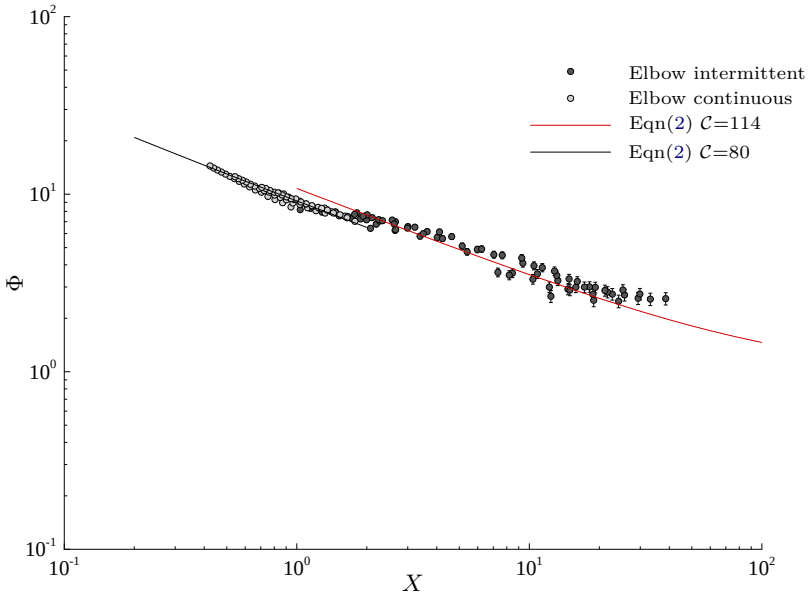

Figure 8: Pressure drop in 90° sharp elbow at different flow patterns.

4 CONCLUSIONS

This work proved the ability of Lockhart-Martinelli method to fit the pressure data across a horizontal 90° sharp elbows for different flow patterns. Further investigations will be conducted in vertically oriented elbows with different pipes diameters.

Acknowledgement

The authors are highly acknowledged the financial support for this work by the Iraqi Ministry Of Higher Education and Scientific Research.

REFERENCES

[1] C. Brennen, *Fundamentals of multiphase flow*. Cambridge University Press, 2005.

[2] J. Thome, *Engineering data book III*, 2004.

[3] O. Baker, "Simultaneous flow of oil and gas," *Oil and Gas J.*, vol. 53, pp. 185–195, 1954.

[4] J. Mandhane, G. Gregory, and K. Aziz, "A flow pattern map for gas-liquid flow in horizontal pipes," *Int. J. Multiph. Flow*, vol. 1, no. 4, pp. 537–553, 1974.

[5] L. Cheng, G. Ribatski, and J. Thome, "Two-phase flow patterns and flow-pattern maps: fundamentals and applications," *Applied Mech. Rev.*, vol. 61, no. 5, p. 050802, 2008.

[6] R. Lockhart and R. Martinelli, "Proposed correlation of data for isothermal two-phase, two-component flow in pipes," *Chem. Eng. Prog.*, vol. 45, no. 1, pp. 39–48, 1949.

[7] D. Chisholm, "A theoretical basis for the Lockhart-Martinelli correlation for two-phase flow," *Int. J. Heat and Mass Transfer*, vol. 10, no. 12, pp. 1767–1778, 1967.

[8] S. Qiao, D. Mena, and S. Kim, "Inlet effects on vertical-downward air–water two-phase flow," *Nuclear Eng. and Design*, vol. 312, pp. 375–388, 2017.

[9] S. Kim, J. Park, G. Kojasoy, and J. Kelly, "Local interfacial structures in horizontal bubbly flow with 90-degree bend," *Int. Conf. Nuclear Eng.*, vol. 2, pp. 219–226, 2006.

[10] R. Kong and S. Kim, "Characterization of horizontal air–water two-phase flow," *Nuclear Eng. and Design*, vol. 312, pp. 266–276, 2017.

[11] K. Mishima and T. Hibiki, "Some characteristics of air-water two-phase flow in small diameter vertical tubes," *Int. J. Multiphase flow*, vol. 22, no. 4, pp. 703–712, 1996.

[12] T. Zhao and Q. Bi, "Pressure drop characteristics of gas–liquid two-phase flow in vertical miniature triangular channels," *Int. J. of Heat and Mass Transfer*, vol. 44, no. 13, pp. 2523–2534, 2001.
[13] H. Lee and S. Lee, "Pressure drop correlations for two-phase flow within horizontal rectangular channels with small heights," *Int. J. Multiphase Flow*, vol. 27, no. 5, pp. 783–796, 2001.
[14] S. Kim, G. Kojasoy, and T. Guo, "Two-phase minor loss in horizontal bubbly flow with elbows: 45-degree and 90-degree elbows," *Nuclear Eng. and Design*, vol. 240, no. 2, pp. 284–289, 2008.
[15] E. Lemmon, M. Huber, and M. McLinden, "NIST Standard Reference Database 23: Reference Fluid Thermodynamic and Transport Properties - REFPROP. 9.0." 2010.

A NOMENCLATURE

Abbreviations

$\mathcal{C}$	Lockhart-Martinelli experimental constant
BSL	Best straight fit line
D^*	Pipe diameter
FPS	Camera speed, Frames per second
FS	Full scale
j	Superficial velocity
LPM	Liters per minute
P^*	Pressure
Re	Reynolds number
$SLPM$	Standard liters per minute
Z^*	Length

Greek symbols

Φ	Two-phase flow multiplier

Scripts

a	Air
F	Liquid-phase
G	Gas-phase
k	Flow phase
TP	Two-phase
w	Water